Iranian Journal of Fuzzy Systems

Volume 22, Number 2, (2025), pp. 171-186

Original paper

University of Sistan and Baluchestan

Fractional fuzzy inference system design and implementation for temperature control

J. M. Atenyi [1] and C. J. Wang [2]

[1, 2] *College of Electrical Engineering and Automation, Shandong University of Science and Technology, Qingdao*

johannatenyi719@gmail.com, cxjwang@sdust.edu.cn

Abstract

Precise temperature regulation is essential in various industrial applications, particularly in environments requiring high accuracy and stability, such as egg incubation. Conventional control strategies, including Proportional-Integral-Derivative (PID) controllers and Fuzzy Inference Systems (FIS), often exhibit limitations in handling nonlinearities, disturbances, and uncertainties. To address these challenges, this research proposes a Fractional Fuzzy Inference System-based PID (FFIS-PID) controller, which enhances the adaptability and robustness of temperature control mechanisms. Unlike traditional fuzzy systems that rely solely on membership degrees, FFIS introduces fractional membership functions and fractional indices, enabling a more flexible and dynamic interpretation of fuzzy rules. The key innovation lies in the fractional compositional rule of inference, which allows the system to intelligently balance the influence of rules by adjusting their impact based on both the truth degree and the information volume. This enhances the adaptability of the control strategy without altering the fundamental rule base structure. The study involves designing fractional membership functions, selecting optimal fractional indices, and evaluating their effects on system behavior. A comparative analysis between FIS-PID and FFIS-PID controllers is conducted through simulations and experimental validation on an incubator system. The results confirm that the FFIS-PID controller provides superior temperature regulation by enabling real-time adaptability to changing conditions. This work contributes to the field of intelligent control by providing a novel approach to fuzzy inference enhancement through fractional compositional rule of inference mechanism. Future research could extend this methodology to other nonlinear control applications, further leveraging fractional indices for improved decision-making and stability.

Keywords: Control strategy, precise temperature control, fractional fuzzy inference system (FFIS), real-world testing.

1 Introduction

Temperature regulation is a fundamental aspect of various industrial processes, where precise control is essential for optimal outcomes. Many temperature-sensitive applications require the maintenance of a narrow temperature range, as even minor deviations can result in significant consequences such as reduced product quality, increased wastage, and compromised efficiency. Consequently, maintaining accurate temperature control is crucial for ensuring operational success in industries like food processing, pharmaceuticals, and electronics manufacturing.

Fuzzy logic control, pioneered by Mamdani's Fuzzy Inference System (FIS) in the 1970s, revolutionized control theory by enabling decision-making under uncertainty. Studies demonstrate fuzzy logic controllers (FLCs) effectively regulate egg incubator conditions: Maulana et al. [7] achieved stabilization of humidity (302s) and temperature (342s), while Lourençoni et al. [2] showed FLCs outperform traditional methods in stability and energy efficiency. Mendoza and Yu [12] highlighted FLCs' capability in managing system uncertainties and non-linearities.

Over decades, FIS evolved into variants like Larsen's product-based translation rules and Takagi-Sugeno's crisp consequents, laying the groundwork for hybrid systems such as Fuzzy-PID (FPID) controllers. FPID integrates fuzzy logic

Corresponding Author: C. J. Wang

Received: June 2024; Revised: March 2025; Accepted: April 2025.

https://doi.org/10.22111/ijfs.2025.48170.8600

with proportional-integral-derivative control to automate gain tuning, achieving superior performance in applications ranging from incubator temperature regulation [1, 6, 15] to other control systems [4, 5, 14]. For instance, Al-Amin and Islam [1] demonstrated FPID's stability in furnace systems, while Liu et al. [6] showcased its rapid convergence in battery thermal systems. Other studies highlight fuzzy PID controllers' efficacy: Kumari and Mohan [5] developed a Mamdani FPID using non-uniform fuzzy sets; Muhammad et al. [14] created a self-tuning FPID for boiler water control in nonlinear systems; Duan et al. [4] applied fuzzy adaptive PID for precise temperature regulation in burn-in tests under disturbances. Despite these successes, FPID systems face persistent limitations in dynamic environments, highlighting the need for more robust frameworks.

The advent of FFISs, which enhance traditional fuzzy inference mechanisms, provides a promising solution for handling complex decision-making in uncertain environments. By incorporating fractional membership functions and fractional indices, systems can dynamically adjust the influence of rules and manage the 'information volume' within fuzzy sets. Building on this, Mazandarani's Fractional Fuzzy Inference System (FFIS) [10] introduces fractional membership functions governed by indices (α^*, β^*) that dynamically modulate the "information volume" of fuzzy sets.

Unlike conventional FISs, which fix membership functions statically, FFIS adjusts their influence based on the reaction trajectories map (RTM)—a novel tool that maps system states (e.g., error and change in error) to optimal fractional indices. For example, in egg incubation systems, small temperature deviations ($\mu^* \approx 0$) activate conservative indices ($\alpha^* = 0.5$), while large errors ($\mu^* \approx 1$) trigger aggressive scaling ($\beta^* = 0.9$) to expedite convergence. Crucially, FFIS generalizes classical FISs: as fractional indices approach unity, FFIS reduces to Mamdani's or Larsen's systems, while optimized indices guarantee superior performance [10]. Recent studies highlight the versatility and growing importance of Fractional Fuzzy Inference Systems (FFIS), especially in complex control scenarios. These systems are designed to incorporate fractional-order dynamics into traditional fuzzy inference, providing enhanced robustness in uncertain or dynamic environments. Mazandarani and Xiu [11] introduced Interval Type-2 Fractional Fuzzy Inference Systems (IT2FFIS), which extend the traditional fuzzy inference systems by incorporating fractional membership functions and reasoning rules. Their work emphasized the potential of IT2FFIS to offer improved adaptability and precision, especially in situations where uncertainty and ambiguity need to be addressed more effectively. Cengiz et al. [3] explored the performance of FFIS in high-order control systems, comparing it with classical fuzzy controllers and PID controllers. Their findings demonstrated that FFIS provides a more effective control strategy, particularly in systems where conventional tuning methods face limitations. The study highlighted FFIS's ability to improve system performance, especially when fine-tuned through genetic algorithms. Mazandarani and Jianfei [8] proposed the Q-Fractionalism Reasoning Learning Method, which combines FFIS with Q-learning to create a system capable of adaptive decision-making. By applying FFIS to real-time position control in a linear switched reluctance motor (LSRM), the method significantly improved the accuracy of control objectives by around 70%, outperforming traditional fuzzy inference systems (FIS) under the same conditions. Mazandarani et al. [9] presented a theoretical explanation for the effectiveness of fractional fuzzy inference in control systems. Their work demonstrated that FFIS, through careful tuning of fractional parameters, can provide up to 40% improvement in system performance. This study underscored the practical benefits of FFIS without delving into fractional calculus, focusing instead on the inherent flexibility and performance enhancements afforded by fractional reasoning techniques. Lastly, Mirzaee and Kazemi [13] demonstrated the effectiveness of a Type-II Fuzzy Inference System-Based Fractional Terminal Sliding Mode Control for zero-force exoskeleton robots. This method, which dynamically adjusts rule impacts to handle uncertainties, showcases the broader adaptability of FFIS in complex, real-time systems. Their work highlights FFIS's potential in applications ranging from robotics to temperature regulation, supporting the idea that FFIS can enhance system robustness and performance under a variety of dynamic conditions.

2 Methodology

2.1 Equipment overview

2.1.1 Arduino board

At the heart of our computational infrastructure is the Arduino Nano ESP32, where the intricate dance of control strategies unfolds. We utilized the Arduino IDE as our coding platform, leveraging its user-friendly interface and robust functionalities to craft and deploy the control algorithm. The Arduino Nano ESP32 is the microcontroller responsible for running the FFIS algorithm and controlling the PWM heating element. The control logic is implemented in C++ and uploaded to the Arduino using the Arduino IDE. Its high processing capability allows real-time computation of the control signals required by the FFIS algorithm.

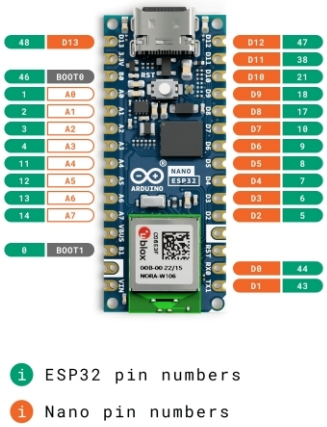

Figure 1: Arduino Nano ESP32 Board.

2.1.2 Temperature sensing with TMP117

Accurate temperature sensing is crucial for the success of the control system. The TMP117 sensor was chosen for this experiment due to its high accuracy (±0.1°C) and low power consumption, which are critical for precise temperature regulation in real-time control systems.

Importance of TMP117: The TMP117 plays a central role in this experiment, as the control system heavily relies on real-time temperature feedback. Its precision ensures that even minor deviations in temperature are detected and corrected promptly by the control system, thus improving the overall performance of the SMC strategy.

I2C Communication: The TMP117 communicates with the Arduino Nano ESP32 via the I2C protocol, ensuring reliable and efficient data transfer. This allows the control system to receive accurate temperature readings in real time and adjust the heating element's power accordingly.

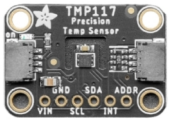

Figure 2: TMP117 Temperature Sensor.

TMP117 is a high-precision digital temperature sensor that utilizes I2C communication, requiring only two pins for data communication (along with one pin for GND and one for power supply).

Accuracy: ±0.1°C.

Resolution: 16-bit resolution for precise measurements.

Temperature Range: −55°C to +155°C.

2.1.3 220V AC PWM duty cycle module

To regulate the heating element, the system employs a 220V AC dimming module controlled through the PWM signal generated by the Arduino Nano ESP32, as shown in Figure 3. The duty cycle of the PWM signal determines the amount of power delivered to the heating element, thereby controlling the rate of heat generation.

The PWM control strategy ensures smooth and efficient power modulation, which is critical for maintaining precise temperature regulation. By varying the duty cycle, the system dynamically adjusts the power to the heating element, providing the necessary heating to achieve and maintain the set temperature.

Product Model: YYAC-3S. It utilizes an original SCR (Silicon Controlled Rectifier) and features complete isolation between the input and output optocouplers, ensuring safe usage with full electrical isolation.

Product Function: It employs a microcontroller with 10 ports to output PWM signals, allowing for adjusting the duty cycle to modify the 220V AC voltage. This enables dimming, speed control, and power regulation, among other purposes.

Figure 3: 220V AC PWM Duty Cycle Module.

Output Power: It can control loads up to 220V and 3A, which corresponds to a maximum power of 660W. Please note that a certain load is required for proper voltage regulation.
Microcontroller Voltage, Frequency, Duty Cycle:
Voltage: Universal range of 3.3V to 5V.
Frequency: 1Hz to 500Hz.
Duty Cycle: 0% to 100%.
PWM input at 0V (low level): Output is 0V.
PWM input at 5V: Output is 220V.

2.1.4 Heated container

As shown in Figure 4, our experimental milieu was a specially chosen small heated container. With foam walls providing insulation and a cotton-covered top, it formed a controlled environment conducive to our study. A heater within the container, complemented by a poly bag containing water, served as the system's heating elements. The incubator is of dimensions of 30 cm (width) × 30 cm (depth) × 65 cm (height) and an internal volume of approximately 58.5 liters.

Figure 4: Heated container with heater and sensor.

Following a comprehensive analysis of the system's behavior, we can express the mathematical model representing heat transfer dynamics. This equation captures the complex relationships governing heat transfer processes within the system.

2.2 Simulation environment

In preparation for conducting simulations, meticulous configuration of the Simulink model is imperative to ensure an accurate representation of the operational conditions and scenarios specific to egg incubation. This entails a thorough definition of key parameters, such as initial temperature conditions, the incorporation of a faithful representation of the egg incubator (whether through a mathematical model or a Simscape model), and identification of potential disturbances that could impact temperature regulation. By meticulously modeling the incubation environment, simulations can yield valuable insights into how the control system responds to real-world challenges. The integration of a Simscape model proved indispensable in our development process, as it meticulously captured the dynamic behavior of the system, particularly its heating mechanisms through radiation. Through the Simulink simulation process, we play a critical role in developing and validating control strategies tailored for egg incubation systems. By carefully configuring the model, employing dual-temperature sensing approaches, and utilizing Simscape for accurate system representation, we gain valuable insights into temperature regulation dynamics. These insights empower us to refine our control algorithms, thereby ensuring optimal performance when deployed in real-world applications.

2.2.1 Thermal behavior and heat transfer equations

Understanding the thermal behavior of systems involves considering various heat transfer mechanisms. The total heat transfer (Q_{total}) within a system can be expressed as:

$$Q_{\text{total}} = Q_{\text{rad}} - Q_{\text{cond}}, \tag{1}$$

where Q_{rad} denotes the heat gained through radiation, and Q_{cond} represents the heat lost through conduction.

Q_{total} can also be represented as

$$Q_{\text{total}} = \rho V C_p \frac{dT}{dt}, \tag{2}$$

where:

- ρ: Density of air (1.184 kg/m^3)
- V: Volume of the incubator (0.058 m^3)
- C_p: Specific heat capacity of air (1006 J/kg°C)
- $\frac{dT}{dt}$: Rate of change of temperature with respect to time

Radiative Heat Transfer (Q_{rad}):

$$Q_{\text{rad}} = A\epsilon\sigma(T_h^4 - T_i^4), \tag{3}$$

where:

- A: Cross-sectional area of the heat source (0.13 m^2)
- ϵ: Emissivity of the heat source (0.95)
- σ: Stefan-Boltzmann constant (5.60×10^{-8} W/m^{2}K^4)
- T_h: Temperature of the heater (50°C)
- T_i: Initial temperature inside the incubator (20°C)

Radiative heat transfer (Q_{rad}) primarily contributes to heating the system, as it represents the influx of thermal energy from the radiating surface to the surroundings.

Conductive Heat Loss (Q_{cond}):

$$Q_{\text{cond}} = \frac{kA\Delta T}{d}, \tag{4}$$

where:

- k: Thermal conductivity of foam (0.030 W/(m·K))
- A: Surface area
- ΔT: Temperature difference across the material
- d: Thickness of the material

Conductive heat loss (Q_{cond}) represents the thermal energy dissipated from the system to its surroundings through conduction. This process tends to cool down the system, as it involves heat transfer away from the surface.

By combining Equations (3), (4), and (2) into (1), and considering the differentials, we arrive at the following expression:

$$\rho V C_p \frac{dT}{dt} = A\epsilon\sigma(T_h^4 - T_i^4) - \frac{kA\Delta T}{d}. \tag{5}$$

The derived mathematical model offers a thorough characterization of the system's dynamics, enabling us to faithfully recreate its behavior within the Simscape simulation framework, as depicted in Figure 5. It is crucial to acknowledge the inherent complexity of the system's operation; however, the developed mathematical model strives to encapsulate the essential aspects of its behavior, providing a sufficient foundation for the design of an effective control strategy.

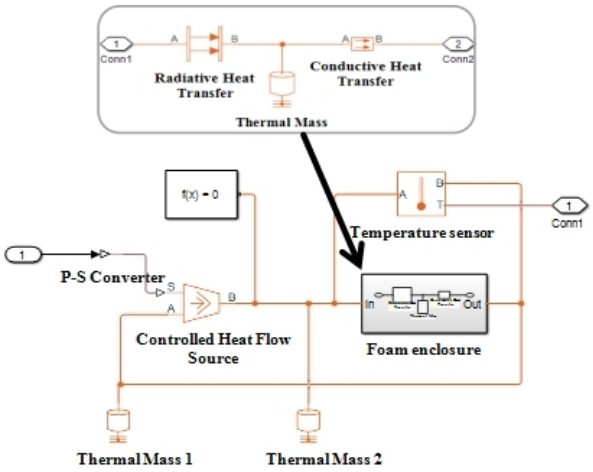

Figure 5: Simscape model of the egg incubator system.

2.3 Fuzzy-PID controller integration: Design and implementation

The Fuzzy Logic Controller (FLC) consists of three main components: input, processing, and output terms. The input term includes *error* (e) and *changing error* (ec), while the output term represents the system's temperature. The processing term uses fuzzy logic rules implemented through if-then statements, where the *if* statement is termed *precursory* and the *then* statement is denoted as *pursuant*. Fuzzification derives fuzzy sets for input variables, and defuzzification yields three parameters: K_p, K_i, and K_d, which enhance the PID control. The FLC rule governs the manipulation of these output variables to optimize system performance. The Membership Table with ranges is shown in Table 1, and the fuzzy logic rules are exemplified in Tables 2, 3, and 4. These rules provide a structured framework for interpreting the relationships between input parameters and the resulting output, enabling the FLC to navigate the complex dynamics of the system and ensure a responsive and adaptive control mechanism.

Table 1: Membership Table with ranges

	NB	NM	NS	ZO	PS	PM	PB
E	[0 0 7]	[0 5 15]	[7 15 20]	[15 20 25]	[20 25 30]	[25 35 40]	[35 40 40]
EC	[-30 -20 -10]	[-20 -10 0]	[-10 0 10]	[5 10 15]	[10 17 30]	[20 30 40]	[30 40 40]
K_p	[-4 -3 -2]	[-3 -2 -1]	[-2 -1 0]	[-1 0 1]	[0 1 2]	[1 2 3]	[2 3 4]
K_i	[-0.08 -0.06 -0.04]	[-0.06 -0.04 -0.02]	[-0.04 -0.02 0]	[-0.02 0 0.02]	[0 0.02 0.04]	[0.02 0.04 0.06]	[0.04 0.06 0.08]
K_d	[-0.4 -0.3 -0.2]	[-0.3 -0.2 -0.1]	[-0.2 -0.1 0]	[-0.1 0 0.1]	[0 0.1 0.2]	[0.1 0.2 0.3]	[0.2 0.3 0.4]

Table 2: Fuzzy Rules for K_p

E/EC	NB	NM	NS	ZO	PS	PM	PB
NB	NM	PB	PB	PM	PM	ZO	ZO
NM	PB	PM	PM	PS	PS	ZO	NM
NS	NM	PM	PM	PS	ZO	NS	NM
ZO	PM	PM	PS	ZO	NS	NM	NM
PS	PS	PS	ZO	NS	NS	NM	NM
PM	PS	ZO	NS	NS	NS	PM	PM
PB	ZO	PS	NM	NM	NM	NB	NB

Table 3: Fuzzy Rules for K_i

E/EC	NB	NM	NS	ZO	PS	PM	PB
NB	NB	NM	NM	PS	ZO	ZO	ZO
NM	PS	NB	NS	NS	NS	ZO	NS
NS	NM	NS	PS	NS	ZO	NS	NS
ZO	NM	NS	NS	ZO	PS	NS	NS
PS	NS	NS	ZO	PS	PM	NM	PM
PM	ZO	NS	PS	PS	PB	NB	NB
PB	ZO	PS	PM	PM	PM	NB	NB

Table 4: Fuzzy Rules for K_d

E/EC	NB	NM	NS	ZO	PS	PM	PB
NB	NB	NS	NM	NM	ZO	ZO	ZO
NM	NM	NS	NB	PM	NS	ZO	NS
NS	PS	NS	NM	NS	ZO	NS	NS
ZO	ZO	NM	NS	ZO	PS	NM	NM
PS	PS	PB	NS	PS	PM	PM	NB
PM	PM	PB	NS	PS	PM	PM	NB
PB	PB	PB	PM	PM	PM	NB	NB

The integration of the Fuzzy-PID controller in Simscape relies on a meticulously crafted rule base and linguistic variables like temperature error (e) and error rate (ec) to dynamically adjust power output for optimal temperature control. This integration, as illustrated in Figure 6, ensures real-time decision-making, enhancing precision and adaptability in temperature regulation.

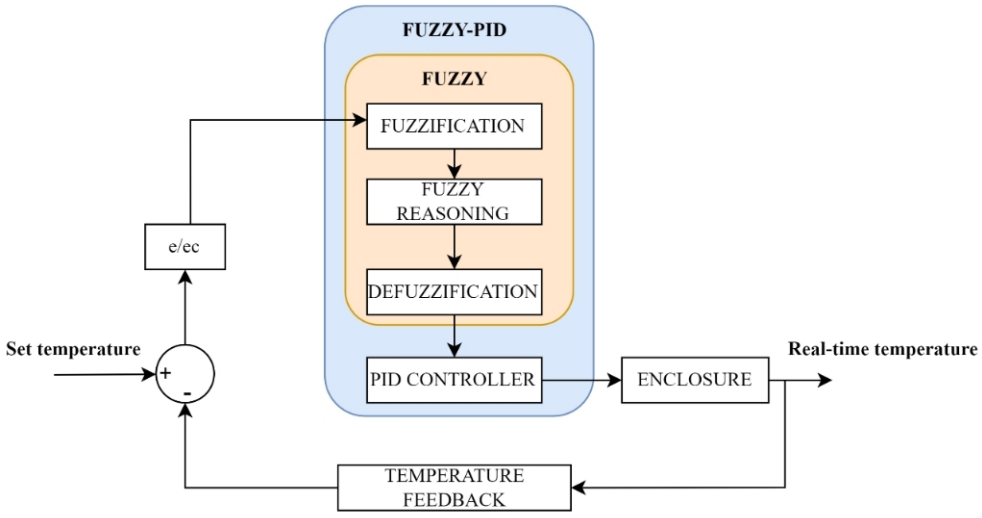

Figure 6: Fuzzy-PID structure diagram for temperature regulation.

2.4 Fractional fuzzy inference system (FFIS) design

The Fractional Fuzzy Inference System (FFIS) is an advanced extension of conventional fuzzy inference systems (FIS), incorporating fractional compositional rule of inference mechanism to enhance accuracy, adaptability, and robustness. This approach modifies traditional fuzzy logic by introducing fractional membership functions, enabling finer control over inference rules and decision-making.

2.4.1 Theoretical foundation

Conventional FIS vs. Fractional FIS

In traditional fuzzy logic systems, membership functions are defined within the range $[0, 1]$, representing the degree of truth of an input variable. FFIS introduces fractional membership functions that allow intermediate degrees of truth, which can be controlled via fractional indices.

Fractional Membership Functions

Fractional membership functions modify conventional membership functions by introducing a parameter called fractional index parameter, allowing more precise representation of uncertainty.

Generalized Fractional Membership Function:

$$A_H(\mu, \alpha_A) = \underline{A}_\mu + \left(\overline{A}_\mu - \underline{A}_\mu\right) \alpha_A, \tag{6}$$

where:

- $\underline{A}_\mu$ and $\overline{A}_\mu$ are the lower and upper bounds of the membership function
- α_A is the fractional index $(0 \leq \alpha_A \leq 1)$

Two primary types of fractional indices are:

- α-type fractional index: Scales membership from the lower bound
- β-type fractional index: Scales membership from the upper bound

For a β-type fractional membership function:

$$A_H(\mu, \beta_A) = \overline{A}_\mu - \left(\overline{A}_\mu - \underline{A}_\mu\right) \beta_A. \tag{7}$$

2.4.2 FFIS implementation

Fractional Membership Calculation

The fractional membership degree is computed using:

$$\mu_{\text{fractional}} = \min(\mu, \mu\alpha^*), \tag{8}$$

where α^* controls the fractional scaling of the membership function.

Fractional Compositional Rule of Inference

The FFIS modifies traditional fuzzy inference by incorporating fractional indices into the rule aggregation process:

$$B = \bigcup_{i=1}^{n} H^{-1}\left(B_{ith}(\mu_i, \alpha_{Bi})\right), \tag{9}$$

where:

- $\mu_i = \mu_i$ (Mamdani-style inference)
- α_{Bi} is the fractional index for output membership functions

For Dynamic Indices

For dynamic indices:

$$\alpha_i^* = f(\mu_i^*) = (\mu_i^*)^n, \tag{10}$$

where:

- μ_i^* is the truth degree of the antecedent
- n is typically 2 (quadratic relationship)

Transition from FIS to FFIS

Objective: Enhance the FIS with fractional calculus to develop the FFIS, introducing fractional indices as per Mazandarani and Xiu [11].

Foundational Definitions:

Definition 2.1. *A fuzzy inference system in which the consequent parts of the rule base consist of fractional membership functions is called a Fractional Fuzzy Inference System (FFIS). This suggests that FFIS can be seen as a type of fuzzy if-then rule translation, also viewed as a new machinery of compositional rule of inference known as the fractional compositional rule of inference. This definition opens the door to a more flexible control system, which we adopt to improve temperature regulation by allowing dynamic adjustment of rule consequents in our incubator system.*

Definition 2.2. *The fracture index of a fractional fuzzy inference system of order (r, s), denoted by γ, is defined as: The fracture index is defined as:*

$$\gamma = 1 - (r + s). \tag{11}$$

Where $r, s \in [0, 1]$, and thus $0 \leq \gamma \leq 1$. When all fractional indices are set to 1 (i.e., $\alpha_i^* = 1$, $\beta_i^* = 1$), the FFIS reduces to a typical FIS, with an order such that $r = 1$ and $s = 1$, and fracture index $\gamma = 0$. This equivalence means that a typical FIS (e.g., Mamdani's) is a special case of FFIS where $\gamma = 0$, and as γ approaches zero, the FFIS behavior aligns with FIS. This insight helps us understand how fractional indices introduce novelty while maintaining compatibility.

Note 1: An FFIS corresponds to an FIS if: 1) the FFIS output approaches the FIS output as γ approaches zero, and 2) the outputs coincide when $\gamma = 0$. This correspondence justifies our transition, ensuring a smooth evolution from FIS.

The Fractional Fuzzy Inference System (FFIS) is implemented in two distinct scenarios: 1) utilizing constant fractional indices, and 2) employing dynamical fractional indices. The constant fractional indices, treated as arbitrary values, are illustrated. As outlined in Definitions 2.1 and 2.2, these indices are organized into three sets: the first set defines an FFIS of order $\left(\frac{2}{7}, \frac{2}{7}\right)$ with a fracture index $\gamma \approx 0.4286$, and the second set $\left(\frac{2.8}{7}, \frac{2.5}{7}\right)$ with $\gamma \approx 0.243$. In contrast, the dynamical fractional indices for the left half-plane (LHP) and right half-plane (RHP) membership functions are designed as quadratic functions dependent on the antecedent part truth degree, specifically expressed as $\alpha^* = f(\mu^*) = (\mu^*)^2$ and $\beta^* = f(\mu^*) = (\mu^*)^2$, as depicted in Table 5. Furthermore, the base operator in the FFIS remains consistent with Mamdani's FIS. The outcomes of applying Mamdani's and FFIS approaches are presented further below.

Table 5: Fractional Indices

Fractional indices	Constant Set #1	Constant Set #2	Dynamic Set #3
β^*_{PB}	0.9	0.5	μ^{*2}
β^*_{PM}	0.8	0.95	μ^{*2}
β^*_{PS}	0.8	0.95	μ^{*2}
α^*_{Z}	1	0.5	μ^{*2}
α^*_{NS}	0.7	0.5	μ^{*2}
α^*_{NM}	0.6	0.5	μ^{*2}
α^*_{NB}	0.5	0.5	μ^{*2}

3 System integration

3.1 Wiring and connections

The seamless integration of various components within our project was fundamental to its success, necessitating a meticulous approach to configuring wiring and connections. This integration primarily revolved around establishing a cohesive interaction among the Arduino board, temperature sensors, and the power regulation module. Our objective was to create a robust and efficient interface capable of effectively orchestrating the operation of the entire system. In Figures 1, 3, and 2, we emphasized illustrating the pathways between key components, including the Arduino Nano ESP32 board, temperature sensor (TMP117), and the power regulation module (220V AC dimming module/PWM duty cycle). Each connection and component were meticulously labeled and defined to facilitate a clear understanding of the electrical architecture.

Functionally, the Arduino Nano ESP32 board served as the central control unit, responsible for orchestrating the operation of the entire system. Its seamless communication with the temperature sensors enabled real-time monitoring and data acquisition, enhancing the system's responsiveness to environmental changes. Simultaneously, the power regulation module played a crucial role in managing and adjusting the power supply, incorporating advanced functionalities such as AC dimming, voltage regulation, speed regulation, and SCR operations. This detailed circuit schematic served not only as a reference during the assembly phase but also as a valuable asset for troubleshooting and potential

Figure 7: Arduino Nano ESP32 schematic.

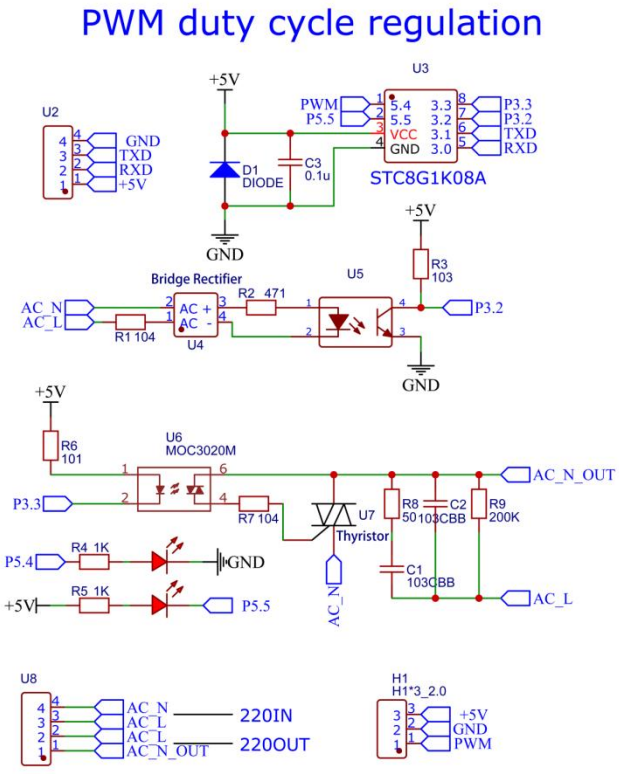

Figure 8: 220V AC PWM duty cycle module schematic.

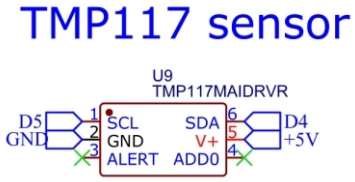

Figure 9: TMP117 schematic.

future modifications. Its comprehensive depiction of the wiring configurations and component connections provided an essential guide for engineers, technicians, and enthusiasts engaged with the system. The thoughtful consideration and meticulous planning invested in the seamless integration of these components significantly contributed to the reliability and functionality of the overall project. Through careful attention to detail, we ensured that our system was not only robust but also flexible and adaptable to potential modifications or enhancements in the future.

3.2 Real-world implementation

Drawing upon insights gleaned from computer simulations, we proceeded to implement our control strategy on an Arduino board for real-world validation. Our system was tailored to regulate temperature within a container equipped with an internal heating system, requiring a sophisticated control algorithm and the integration of dual temperature sensors.

The experimental setup included the Arduino Nano ESP32 as the central controller, the TMP117 sensor for temperature feedback, the PWM module for controlling the heating element, and the Arduino IDE code to implement the control algorithm. Figure 10 depicts the experimental setup. The heating mechanism employed entails warming water contained within a poly bag, with heat radiation serving to effectively raise the interior temperature of the system. Central to our real-world implementation is the collaborative interplay between this internal heating system and the feedback obtained from temperature sensors. This integrative approach, which harmonizes simulated insights with practical considerations, situates our research at the nexus of precise theoretical modeling and pragmatic real-world functionality. The experimental setup for our real-world implementation, showcased in Figure 10, includes all components utilized in constructing and rigorously testing the system, embodying our commitment to methodical experimentation and validation.

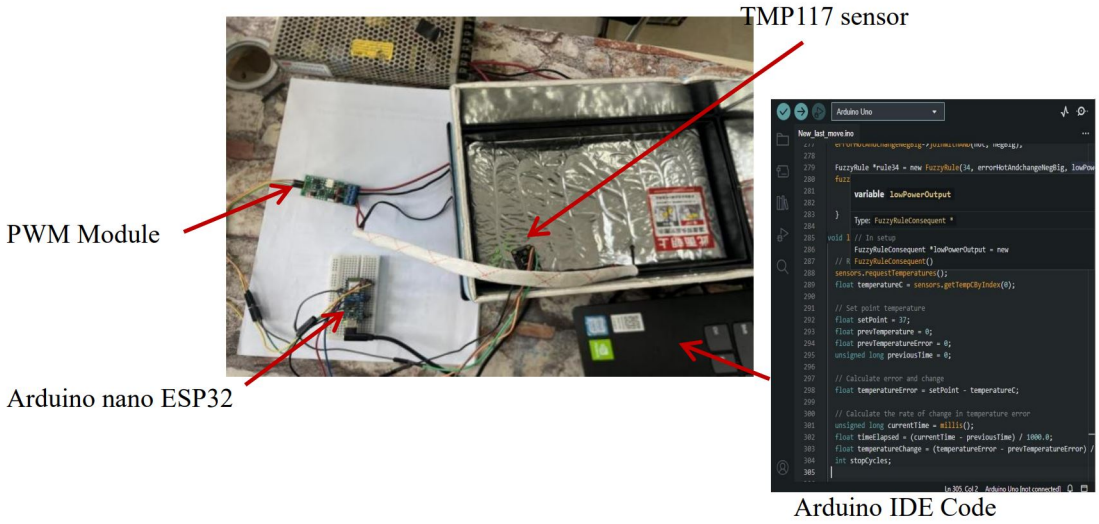

Figure 10: Experimental setup.

4 Simulation and results analysis

In this section, we present a detailed analysis of the simulation results obtained for the FFIS-PID and Fuzzy-PID controllers applied to temperature regulation in egg incubators. Through this comparative analysis, we aim to evaluate the controllers' effectiveness in maintaining precise temperature control and assess their robustness in the presence of disturbances.

4.1 Simulation results

As illustrated in Figure 11, a comparative analysis of FFIS-based control methods—SET#1, SET#2, SET#3, and Fuzzy-PID—against a target setpoint of 37.5°C, with MATLAB simulation results illustrating their performance.

SET#1 achieves the fastest stabilization, reaching the setpoint within approximately 20–30 seconds with minimal overshoot, highlighting an optimally tuned FFIS configuration that effectively balances feedforward, integral, and state feedback components. In contrast, SET#2 and SET#3 exhibit a slower convergence, stabilizing around 30–40 seconds, with smoother trajectories that suggest a more conservative tuning approach, potentially prioritizing stability over speed in response to varying conditions. Fuzzy-PID indicates an adaptive FFIS approach, but its overshoot suggests the fuzzy rules or membership functions may need refinement to match the setpoint more closely. All methods are derived from different FFIS indices, which serves as a baseline for these simulations. Among the evaluated methods, SET#1 stands out as the most effective, offering the best combination of rapid response and accuracy, making it a promising candidate for real-world applications requiring efficient temperature regulation.

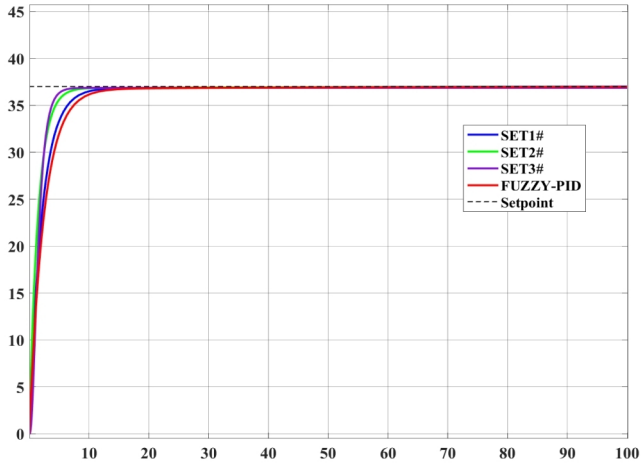

Figure 11: Combined graph comparing SET#1, SET#2, SET#3, and Fuzzy-PID at a 37.5°C setpoint.

4.2 Real-world implementation results

4.2.1 Comparison of control ability: FFIS-PID vs. Fuzzy-PID

In this subsection, we perform a detailed comparison between FFIS-PID and Fuzzy-PID control strategies for a temperature setpoint of 37.5°C.

Figure 12 demonstrates the response of the system controlled by FFIS-PID. The FFIS-PID temperature control graph demonstrates a gradual rise from 35.0°C to a stable 37.5°C setpoint over approximately 200–300 seconds, with minor fluctuations thereafter. This indicates effective control with a smooth transition and good steady-state accuracy, likely due to a well-tuned FFIS-PID configuration balancing feedforward and PID components.

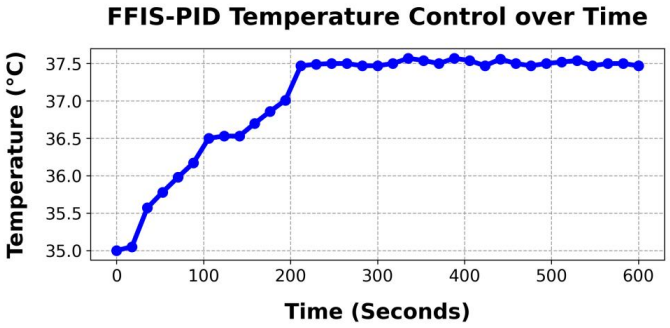

Figure 12: FFIS-PID temperature control over time at a 37.5°C setpoint.

As seen in Figure 13, the Fuzzy-PID temperature control graph shows a steady increase from 35.0°C to 37.5°C, stabilizing around 300 seconds with slight oscillations. This suggests a robust control strategy, though the slower response and minor fluctuations indicate potential room for tuning to enhance precision and reduce settling time.

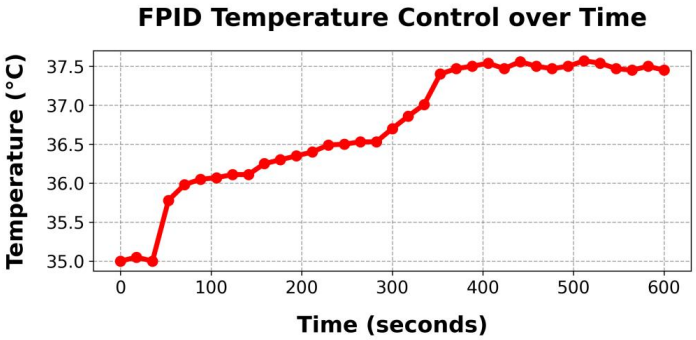

Figure 13: Fuzzy-PID temperature control over time at a 37.5°C setpoint.

As shown in Figure 14, in the comparison of FFIS-PID and Fuzzy-PID temperature control methods, FFIS-PID emerges as the superior approach. It exhibits a smoother rise and maintains closer alignment to the 37.5°C setpoint with reduced variability, as supported by a mean squared error of 0.2327°C^2 and a maximum difference of 1.07°C. Although Fuzzy-PID demonstrates a marginally faster initial response, its higher variability indicates less consistent control. Therefore, FFIS-PID is recommended for applications demanding precise and stable temperature regulation.

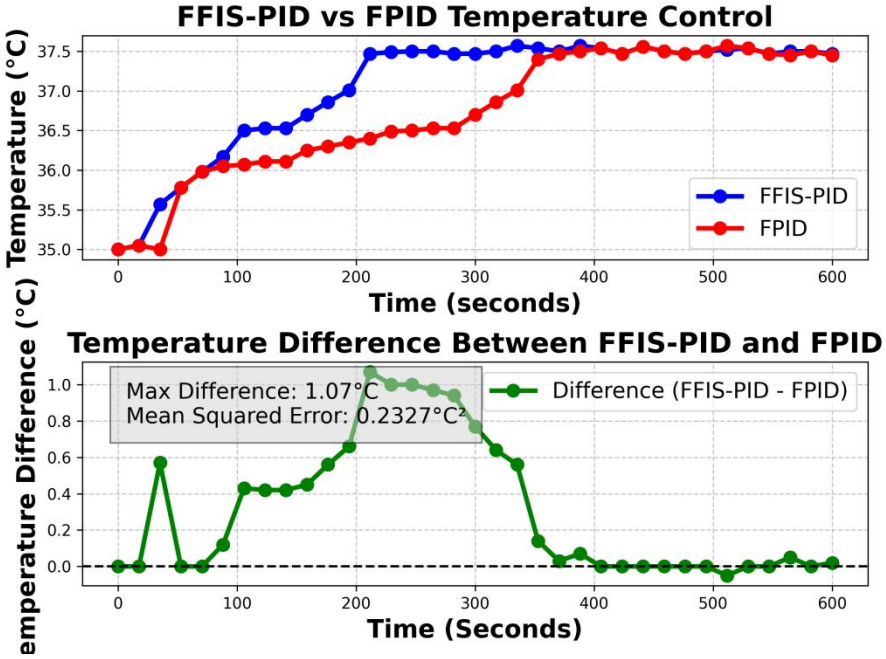

Figure 14: Comparison of FFIS-PID and Fuzzy-PID temperature control at a 37.5°C setpoint.

4.3 Comparison of control signals for FFIS-PID and fuzzy-PID controllers

A comprehensive comparison of the control signals produced by the FFIS-PID and Fuzzy-PID controllers in the context of temperature regulation is presented. The analysis focuses on the performance characteristics of both controllers as they manage temperature within a defined operational range. To facilitate understanding, we include graphical representations that illustrate the differences in performance between the two control strategies.

4.3.1 Graphical analysis

Figure 15 visualizes the 'Control Signal vs Temperature (Comparison)' graph, which compares the control signals of FFIS-PID (blue) and Fuzzy-PID (red) across a temperature range from 35.0°C to 37.5°C. FFIS-PID maintains a lower

and more stable control signal, peaking at a maximum of 2.73, indicative of efficient regulation. In contrast, Fuzzy-PID exhibits higher and more variable signals, reaching up to 6–8, suggesting a less optimized response. The difference plot (green) highlights that Fuzzy-PID's control signal exceeds FFIS-PID's by up to 4 units, underscoring FFIS-PID's superior efficiency and stability in temperature control, making it a preferable choice for precise applications.

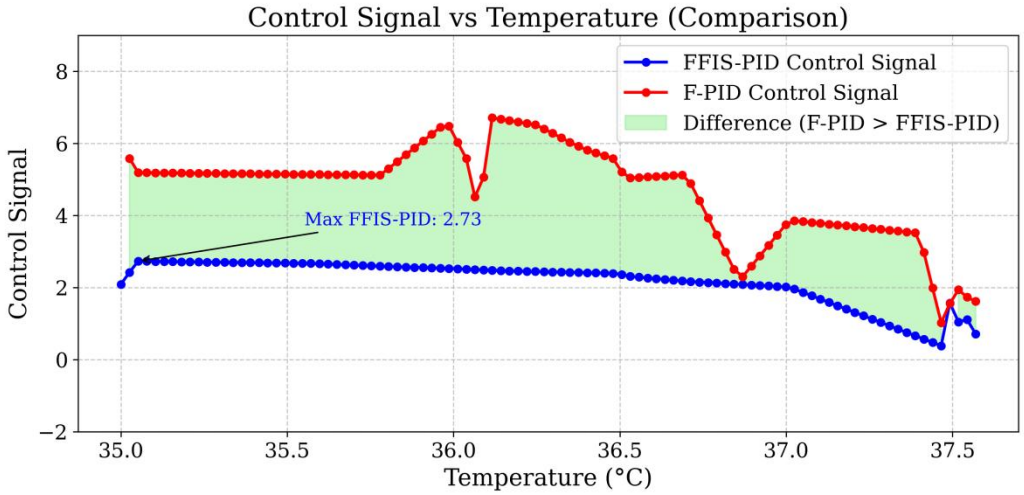

Figure 15: Comparison of control signals for FFIS-PID and Fuzzy-PID across a temperature range of 35.0°C to 37.5°C.

4.3.2 Additional analysis at a setpoint of 30°C

✓ In addition to the analysis conducted at a setpoint of 37.5°C, we also evaluate the performance of both controllers when the target temperature is set to 30°C. This lower temperature setpoint presents an opportunity to analyze the controllers' behavior under varying operational demands.

Figure 16 illustrates the 'FFIS-PID vs Fuzzy-PID Temperature Control' graph, with MATLAB simulation results, comparing the performance of FFIS-PID (blue) and Fuzzy-PID (red) against a 30°C setpoint over 600 seconds. Both methods stabilize near the setpoint, with FFIS-PID showing a slightly smoother and more consistent trajectory, while Fuzzy-PID exhibits minor oscillations. The difference plot (green) reveals a maximum temperature difference of 0.60°C and a mean squared error of 0.0433°C^2, indicating that FFIS-PID maintains a closer alignment to the setpoint with greater precision. This suggests FFIS-PID is the more effective control strategy for achieving stable and accurate temperature regulation at this setpoint.

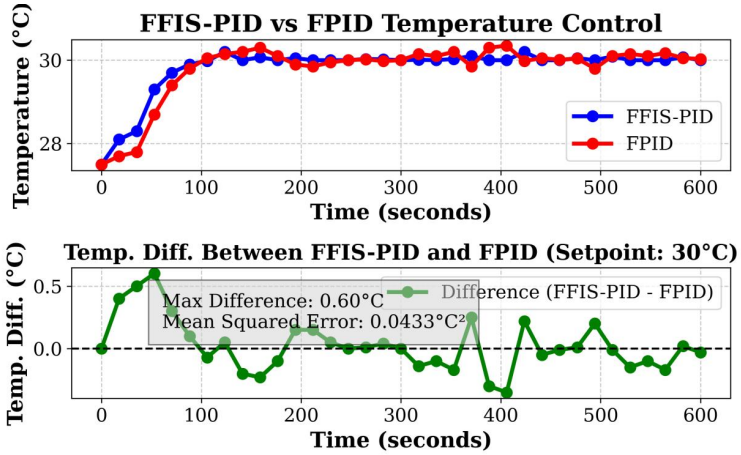

Figure 16: Comparison of FFIS-PID and Fuzzy-PID temperature control at a 30°C setpoint.

5 Conclusion

This thesis has provided a comprehensive evaluation of FFIS-PID and Fuzzy-PID controllers for temperature regulation in egg incubators, with the initial MATLAB simulation results in section 4 offering a comparative analysis of FFIS-based methods (SET#1, SET#2, SET#3, and Fuzzy-PID) against a 37.5°C setpoint. SET#1 stood out, achieving the fastest stabilization (20–30 seconds) with minimal overshoot, attributed to its optimally tuned feedforward, integral, and state feedback components. SET#2 and SET#3, with slower convergence (30–40 seconds) and smoother trajectories, suggested a conservative tuning approach suited for stability-focused scenarios. Fuzzy-PID, despite its adaptive design, exhibited moderate overshoot and slower settling (around 50 seconds), indicating a need for refinement in its fuzzy logic parameters.

Real-world implementation results, specifically based on a comparison of SET#1 (as the FFIS-PID representative) versus Fuzzy-PID, further validated these findings. SET#1 demonstrated a gradual rise to 37.5°C over 200–300 seconds with minor fluctuations, reflecting effective control and strong steady-state accuracy. In contrast, Fuzzy-PID showed a slower stabilization (around 300 seconds) with slight oscillations, suggesting potential for tuning to improve precision. The direct comparison at 37.5°C, supported by a mean squared error of $0.2327°C^2$ and a maximum difference of 1.07°C, confirmed SET#1's superior stability and accuracy. The control signal analysis reinforced this, with SET#1 maintaining a lower peak signal (2.73) compared to Fuzzy-PID's higher and more variable signals (up to 6–8), highlighting its efficiency.

At a 30°C setpoint, real-world data showed SET#1 maintaining a smoother trajectory with a mean squared error of $0.0433°C^2$ and a maximum difference of 0.60°C, outperforming Fuzzy-PID's oscillatory response. These results underscore SET#1's robustness and precision across varying conditions, establishing it as the preferred control strategy for egg incubator applications. Future research could focus on optimizing FFIS and exploring hybrid approaches to enhance performance under disturbances. This study solidifies FFIS as a reliable and effective solution for precise temperature regulation in agricultural settings.

Acknowledgement

The authors sincerely thank the editor and anonymous referees for their thorough review and valuable suggestions, which greatly improved the clarity of the paper.

References

[1] M. Al-Amin, M. S. Islam, *Design of an intelligent temperature controller of furnace system using the fuzzy self-tuning PID controller*, in 2021 International Conference on Electronics, Communications and Information Technology (ICECIT), IEEE, (2021), 1-4. https://doi.org/10.1109/ICECIT54077.2021.9641467

[2] D. C. T. C. de Brito, P. T. L. De Oliveira, S. H. N. Turco, J. da S. Cunha, *Fuzzy controller applied to temperature adjustment in incubation of free-range eggs*, Engenharia Agrícola, **42** (2022), e20220050. https://doi.org/10.1590/1809-4430-Eng.Agric.v42n4e20220050/2022

[3] M. Cengiz, F. N. Deniz, O. Ozguven, *Comparative performance evaluation of fractional fuzzy inference system for A high-order system*, in 7th International Symposium on Innovative Approaches in Smart Technologies (ISAS), (2023), 1-6. https://doi.org/10.1109/ISAS60782.2023.10391480

[4] Y. Duan, H. Ji, X. Sun, W. Tian, H. Cui, *Design of temperature control system for burn-in test based on fuzzy adaptive PID control algorithm*, in 2022, 23rd International Conference on Electronic Packaging Technology (ICEPT), IEEE, (2022), 1-6. https://doi.org/10.1109/ICEPT56209.2022.9873275

[5] K. Kumari, B. M. Mohan, *Modelling and simulation of a Mamdani fuzzy PID controller using non-uniformly distributed fuzzy sets*, in 2023, 9th International Conference on Control, Decision and Information Technologies (CoDIT), IEEE, (2023), 1-6. https://doi.org/10.1109/CoDIT58514.2023.10284213

[6] Z. Liu, J. Liu, N. Wang, *Thermal management with fast temperature convergence based on optimized fuzzy PID algorithm for electric vehicle battery*, Applied Energy, **352** (2023), 1-10. https://doi.org/10.1016/j.apenergy.2023.121936

[7] Y. Z. Maulana, F. Fathurrohman, G. Wibisono, *Egg incubator temperature and humidity control using fuzzy logic controller*, Jurnal RESTI (Rekayasa Sistem dan Teknologi Informasi), **7** (2023), 318–325. https://doi.org/10.29207/resti.v7i2.4728

[8] M. Mazandarani, P. Jianfei, *The Q-fractionalism reasoning learning method*, IEEE Transactions on Neural Networks and Learning Systems, **36** (2025), 1568-1582. https://doi.org/10.1109/TNNLS.2023.3326376

[9] M. Mazandarani, O. Kosheleva, V. Kreinovich, *Why fractional fuzzy*, in Fuzzy Logic and Technology, and Aggregation Operators, Lecture Notes in Computer Science, **14069** (2023), 285-296. https://doi.org/10.1007/978-3-031-39965-724

[10] M. Mazandarani, X. Li, *Fractional fuzzy inference system: The new generation of fuzzy inference systems*, IEEE Access, **8** (2020), 126066-126082. https://doi.org/10.1109/ACCESS.2020.3008064

[11] M. Mazandarani, L. Xiu, *Interval type-2 fractional fuzzy inference systems: Towards an evolution in fuzzy inference systems*, Expert Systems With Applications, **189** (2022), 115947. https://doi.org/10.1016/j.eswa.2021.115947

[12] A. M. E. R. Mendoza, W. Yu, *Fuzzy adaptive control law for trajectory tracking based on a fuzzy adaptive neural PID controller of a multi-rotor unmanned aerial vehicle*, International Journal of Control, Automation and Systems, **21** (2023), 658-670. https://doi.org/10.1007/s12555-021-0299-2

[13] M. Mirzaee, R. Kazemi, *Type-II fuzzy inference system-based fractional terminal sliding mode control for zero-force exoskeleton robots*, Iranian Journal of Fuzzy Systems, **21** (2024), 147-171. https://doi.org/10.22111/ijfs.2025.49399.8718

[14] Z. Muhammad, S. H. A. Dziauddin, S. A. Hamid, N. A. M. Leh, *Water level control in boiler system using self-tuning fuzzy PID controller*, in 2023 IEEE 13th International Conference on Control System, Computing and Engineering (ICCSCE), IEEE, (2023), 232-237. https://doi.org/10.1109/ICCSCE58721.2023.10237138

[15] M. M. Rahman, M. S. Islam, *Design of a fuzzy based PID algorithm for temperature control of an incubator*, Journal of Physics: Conference Series, **1969** (2021), 1-10. https://doi.org/10.1088/1742-6596/1969/1/012055